University Library

MINERVA ACCESS

A gateway to Melbourne's research publications

Minerva Access is the Institutional Repository of The University of Melbourne

Author/s:
Doherty, MW;Struzhkin, VV;Simpson, DA;McGuinness, LP;Meng, Y;Stacey, A;Karle, TJ;Hemley, RJ;Manson, NB;Hollenberg, LCL;Prawer, S

Title:
Electronic properties and metrology applications of the diamond NV - Center under pressure

Date:
2014-01-31

Citation:
Doherty, M. W., Struzhkin, V. V., Simpson, D. A., McGuinness, L. P., Meng, Y., Stacey, A., Karle, T. J., Hemley, R. J., Manson, N. B., Hollenberg, L. C. L. & Prawer, S. (2014). Electronic properties and metrology applications of the diamond NV - Center under pressure. Physical Review Letters, 112 (4), https://doi.org/10.1103/PhysRevLett.112.047601.

Persistent Link:
https://hdl.handle.net/11343/52501

Electronic Properties and Metrology Applications of the Diamond NV^- Center under Pressure

Marcus W. Doherty,[1,*] Viktor V. Struzhkin,[2] David A. Simpson,[3] Liam P. McGuinness,[3,4] Yufei Meng,[2] Alastair Stacey,[5] Timothy J. Karle,[5] Russell J. Hemley,[2] Neil B. Manson,[1] Lloyd C. L. Hollenberg,[3] and Steven Prawer[5]

[1]*Laser Physics Centre, Research School of Physics and Engineering, Australian National University, Australian Capital Territory 0200, Australia*

[2]*Geophysical Laboratory, Carnegie Institution of Washington, Washington DC 20015, USA*

[3]*Centre for Quantum Computation and Communication Technology, School of Physics, University of Melbourne, Victoria 3010, Australia*

[4]*Institute for Quantum Optics, University of Ulm, D-89081 Ulm, Germany*

[5]*School of Physics and Melbourne Materials Institute, University of Melbourne, Victoria 3010, Australia*

(Received 10 May 2013; published 31 January 2014)

The negatively charged nitrogen-vacancy (NV^-) center in diamond has realized new frontiers in quantum technology. Here, the optical and spin resonances of the NV^- center are observed under hydrostatic pressures up to 60 GPa. Our results motivate powerful new techniques to measure pressure and image high-pressure magnetic and electric phenomena. Additionally, molecular orbital analysis and semiclassical calculations provide insight into the effects of compression on the electronic orbitals of the NV^- center.

DOI: 10.1103/PhysRevLett.112.047601 PACS numbers: 76.70.Hb, 62.50.-p, 61.72.jn

The negatively charged nitrogen-vacancy (NV^-) center is a remarkable point defect in diamond and is the system of choice for a rapidly expanding domain of quantum technology demonstrations, including information processing [1,2], communications [3,4], and metrology [5–14]. The NV^- center is also particularly rich in physics; however, somewhat surprisingly, many fundamental aspects of the center remain unresolved (see Ref. [15] for an extensive review). Indeed, most of the center's applications exploit its unique combination of long-lived ground state spin coherence [16,17] and optical spin polarization and readout that persist to ambient temperatures and beyond [18]. Attainment of a complete understanding of the latter is particularly important to the optimization of the NV^- center's applications as well as to the identification of other useful defects.

Recently, the effects of temperature on the center's ground state spin and optical spin polarization and readout mechanism have been investigated, which enabled the influence of temperature on existing NV^- metrology applications to be characterized and new thermometry applications to be proposed [18–21]. There has been no commensurate investigation of the effects of pressure. Pressure and uniaxial stress enable the lattice and electronic orbitals of the NV^- center to be manipulated, thus providing probes into the center's intriguing coupling of orbital and spin dynamics. Such investigations will complete the characterization of NV^- metrology under extreme conditions and is of particular interest to fields such as high-pressure superconductivity, magnetic and electric phase transitions [22–28]. Here, we present the first observations of the behavior of the ground state spin of the NV^- center under hydrostatic pressure. Our observations provide new insight into the physics of the center, motivate the center as a pressure sensor, and enable an analysis of the center's other metrology applications under extreme conditions.

The NV^- center is a C_{3v} point defect in diamond consisting of a substitutional nitrogen atom adjacent to a carbon vacancy that has trapped an additional electron [refer to Fig. 1(a)]. As depicted in Fig. 1(b), the one-electron orbital level structure of the NV^- center contains three defect orbital levels (a_1, e_x, and e_y) deep within the diamond band gap. EPR observations and *ab initio* calculations indicate that these defect orbitals are highly localized to the center [29–32]. Figure 1(c) shows the center's many-electron electronic structure generated by the occupation of the three defect orbitals by four electrons [33,34], including the zero phonon line (ZPL) energies of the optical (1.945 eV/637 nm) [35] and infrared (1.190 eV/1042 nm) [36–38] transitions. The energy separations of the spin triplet and singlet levels ($^3A_2 \leftrightarrow {}^1E$ and $^1A_1 \leftrightarrow {}^3E$) are unknown.

As depicted in the inset of Fig. 1(c), the ground $^3A_2$ level exhibits a zero field fine structure splitting between the $m_s = 0$ and ± 1 spin sublevels of $D \sim 2.87$ GHz (room temperature), which is principally due to first-order electron spin-spin interaction [39]. While second-order spin-orbit interaction does contribute to the zero field splitting, its contribution is much smaller than that of spin-spin and it can be ignored in this work [15]. The zero field parameter D and spin quantization axis are thus determined by the trigonal unpaired electron spin density distribution of the ground $^3A_2$ level. Under crystal strain that distorts the trigonal symmetry of the center, the degeneracy of the $m_s = \pm 1$ sublevels is lifted. The spin Hamiltonian that describes the $^3A_2$ fine structure is

 © 2014 American Physical Society

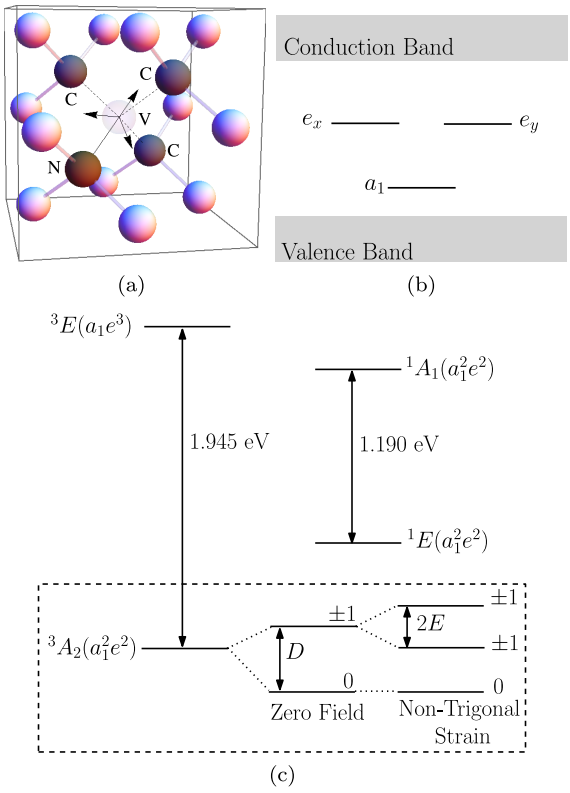


FIG. 1 (color online). (a) Schematic of the NV center depicting the vacancy (transparent), the nearest neighbor carbon atoms (gray), the substitutional nitrogen atom (brown), the next-to-nearest carbon neighbors (white) and the adopted coordinate system (z axis aligned with the trigonal axis of the center). (b) The NV^- one-electron orbital level structure depicting the diamond valence and conduction bands and the three defect orbitals (a_1, e_x, and e_y) within the band gap. (c) Schematic of the center's many-electron electronic structure, including the optical 1.945 eV and infrared 1.190 eV ZPL energies. The electronic configurations of the many-electron levels are indicated in parentheses. Inset: The fine structure of the ground $^3A_2$ level: at zero field with a single splitting of $D \sim 2.87$ GHz; and in the presence of nontrigonal strain, with a further strain dependent splitting denoted by E.

$$H = D[S_z^2 - S(S+1)/3] + E(S_x^2 - S_y^2), \qquad (1)$$

where E is the strain parameter, the $S = 1$ spin operators are dimensionless, and the z coordinate axis coincides with the center's trigonal symmetry axis [see Fig. 1(a)].

The spin of the ground $^3A_2$ level is optically polarized via the combination of optical excitation and spin-selective nonradiative intersystem crossings (ISCs) that preferentially depopulate the $m_s = \pm 1$ sublevels and populate the $m_s = 0$ sublevel [40]. The ISCs also lead to spin-dependent optical fluorescence that enable the ground state spin to be readout and the performance of ground state optically detected magnetic resonance (ODMR) [40]. The dark ISCs of the NV^- center are yet to be fully understood and they are currently believed to be the combined result of spin-orbit coupling of the lowest energy triplet ($^3A_2$, ^3E) and singlet ($^1A_1$, ^1E) levels and electron-phonon decay [40].

In our experiments, we observed the hydrostatic pressure shift of the optical ZPL and the ground state ODMR of small ensembles of NV^- centers at room temperature [41]. As depicted in Fig. 2(a), our experiments were performed in a diamond anvil cell (DAC) using samples of type IIa single-crystal CVD diamond with low nitrogen content (< 1 ppm). The shift of the optical ZPL was measured in NaCl pressure media and detected using a spectrometer. We measure ODMR in two different pressure media: NaCl and Ne. ODMR was performed by optically exciting the NV^- centers with 532 nm light and scanning the microwave frequency through either a current carrying Pt wire embedded in an insulating BN + epoxy gasket or a copper coil wound a few times around one of the diamond culets. We measured the pressure *in situ* using the fluorescence of a small ruby chip located in the DAC [42]. The maximum pressure applied was 60 GPa, which was limited by the blue shift of the NV^- ZPL to the 532 nm optical excitation wavelength. A systematic ODMR temperature shift was avoided in our experiments by allowing the DAC to come to thermal equilibrium in the presence of steady microwave excitation at each pressure.

Figure 3 shows selected ODMR spectra and the observed shift of the splitting parameter D. The shift of D with pressure P is highly linear and has the gradient $dD(P)/dP = 14.58(6)$ MHz/GPa. The broadening and splitting of the ODMR line at > 4.5 GPa are results of crystal distortion. Above > 4.5 GPa, the Ne pressure medium freezes at room temperature and becomes quasi-hydrostatic. As a consequence, the stress applied to the crystal is slightly anisotropic (< 0.4 GPa at 50 GPa) and the crystal distorts [43]. Figure 3 also depicts the observed shift of the optical ZPL energy, which is also highly linear and has the gradient 5.75 meV/GPa. This result compares

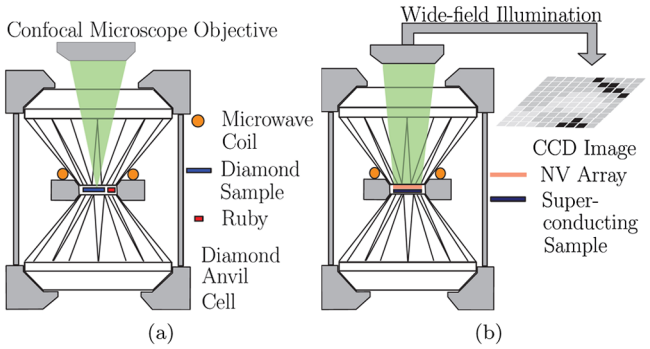


FIG. 2 (color online). (a) Schematic of the DAC arrangement used in our experiments. Diamond samples were placed in the DAC working space together with the hydrostatic pressure medium and a ruby crystal for pressure measurement. The diamond culets provide optical access to optically excite (532 nm) and collect the NV^- redshifted fluorescence. (b) Schematic of the proposed design of a diamond chip containing an NV^- array, which is used to switch between pressure monitoring and wide field imaging of the magnetic field at the surface of a high-pressure superconductor.

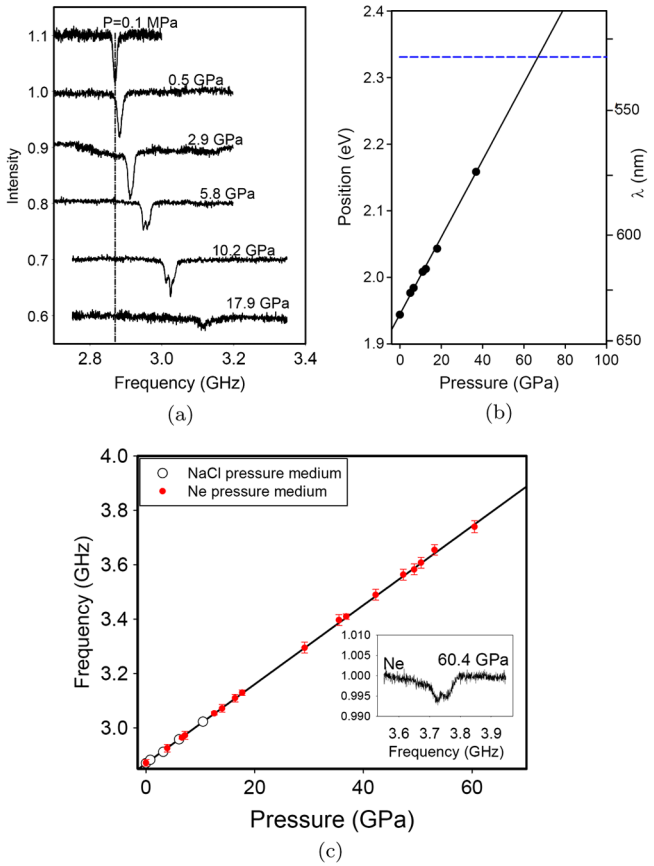


FIG. 3 (color online). (a) Example NV$^-$ ODMR spectra in the quasihydrostatic NaCl pressure medium. The dashed line indicates the position of the resonance at ambient pressure. (b) The pressure shift of the optical ZPL. Solid line is a linear fit extrapolated to the position of the 532 nm excitation laser. (c) The measured ODMR splitting parameter D in quasihydrostatic (NaCl) and hydrostatic (Ne) pressure media up to 60 GPa. D is taken as the midpoint of the two ODMR peaks and error bars correspond to the full width of the ODMR peaks (see Ref. [41] for further details). Inset: the ODMR spectrum in Ne at 60 GPa.

reasonably to a previous measurement of 5.5 meV/GPa obtained from high density ensembles of NV$^-$ centers in type Ib diamond using a N_2 pressure medium [44]. The small difference can be attributed to the significantly inhomogeneously strain broadened optical ZPLs of the high density ensembles and the different quasihydrostatic behavior of N_2 pressure media.

Our hydrostatic pressure ODMR measurements provided a controlled means to probe the electronic orbitals of the NV$^-$ center. Under hydrostatic pressure, the equilibrium positions of the nuclei of the lattice contract and thus, the defect orbitals change. Considering the ground $^3A_2$ level, the change in the defect orbitals corresponds to the contraction of the unpaired spin density of the level, which thereby increases the electronic spin-spin interactions and D. Picturing the defect orbitals as linear combinations of atomic orbitals [39], the contraction of the unpaired spin density maybe seen to have two aspects: (1) the compression of the nuclear lattice decreases the distance between atomic orbitals, and (2) the compression of the nuclear lattice deepens the localizing electrostatic potential of the center, thereby modifying the linear combinations such that the defect orbitals become more localized to the atoms closer to the vacancy. Elaborating on (2), EPR observations and *ab initio* calculations [29–32] indicate that the defect orbitals are combinations of the orbitals of atoms belonging to concentric shells centered on the vacancy, such that the greatest contributions are from the three nearest neighbor carbon atoms of the vacancy. As pressure is increased, it is pictured that the contributions of orbitals of the inner shell atoms increase as the contributions of more distant shell atoms decrease, thereby resulting in a net shift of electron probability density towards the vacancy.

This picture can be demonstrated using the molecular model of the NV$^-$ center [33,34,45], where the spin-spin D parameter of the $^3A_2$ level is given by

$$D = C\langle e_x(\vec{r}_1)e_y(\vec{r}_2)|\frac{1}{r_{12}^3} - \frac{3z_{12}^2}{r_{12}^5}[|e_x(\vec{r}_1)e_y(\vec{r}_2)\rangle - |e_y(\vec{r}_1)e_x(\vec{r}_2)\rangle], \quad (2)$$

where $C = 3\mu_0 g_e^2 \mu_B^2/16\pi h$ is a constant, μ_0 is the permeability of free space, g_e is the free electron g factor, μ_B is the Bohr magneton, h is Planck's constant, $\vec{r}_i = x_i\hat{\vec{x}} + y_i\hat{\vec{y}} + z_i\hat{\vec{z}}$ is the position of the ith electron, $r_{12} = |\vec{r}_2 - \vec{r}_1|$ and $z_{12} = z_2 - z_1$. The dominant contributions to the above expression can be determined by expanding the defect orbitals in terms of their linear combinations of atomic orbitals and retaining just the contributions from the dangling sp^3 atomic orbitals (c_1, c_2, c_3) of the vacancy's three nearest-neighbor carbon atoms. Note that the dangling nitrogen atomic orbital does not contribute to the e defect orbitals [33,34,45]. Applying the symmetry relationships between the carbon orbitals and ignoring orbital overlaps, D is simplified to

$$D \approx C\kappa^2\langle c_1(\vec{r}_1)c_2(\vec{r}_2)|\frac{1}{r_{12}^3} - \frac{3z_{12}^2}{r_{12}^5}|c_1(\vec{r}_1)c_2(\vec{r}_2)\rangle, \quad (3)$$

where κ is the fraction of e orbital probability density associated with the three nearest neighbor carbon atoms. This approximation clearly shows that the dominant contribution to D is a direct integral between the dangling sp^3 electronic densities of the carbon atoms surrounding the vacancy. This direct integral is reduced by the unpaired spin density κ of the e defect orbitals centered on the carbon atoms surrounding the vacancy. Interpretations of EPR studies have estimated $\kappa \sim 0.84$ [30].

Under hydrostatic pressure, the nuclear lattice is isotropically compressed. The normal nuclear displacement coordinate $Q = P/\gamma B$ of hydrostatic compression is connected to the pressure P via the diamond bulk modulus B and a geometric factor γ that relates the hydrostatic volume strain

to the nuclear displacement. The linear pressure shift of D at zero pressure is then

$$\left.\frac{dD}{dP}\right|_0 \approx \frac{C}{\gamma B}\kappa^2|_0 \left.\frac{d}{dQ}\left\langle\frac{1}{r_{12}^3}-\frac{3z_{12}^2}{r_{12}^5}\right\rangle\right|_0 + \frac{C}{\gamma B}\left.\frac{d\kappa^2}{dQ}\right|_0 \left\langle\frac{1}{r_{12}^3}-\frac{3z_{12}^2}{r_{12}^5}\right\rangle|_0, \quad (4)$$

where $\langle(1/r_{12}^3)-(3z_{12}^2/r_{12}^5)\rangle = \langle c_1(\vec{r}_1)c_2(\vec{r}_2)|(1/r_{12}^3)-(3z_{12}^2)/(r_{12}^5)|c_1(\vec{r}_1)c_2(\vec{r}_2)\rangle$. As pictured, the first line accounts for the displacements of the atomic orbitals, whereas the second line accounts for the change in the unpaired spin density κ centered on the carbon atoms.

A semiclassical calculation yields the following estimate of the shift due to the displacement of the atomic orbitals (see Ref. [41] for further details),

$$\frac{C}{\gamma B}\kappa^2|_0 \left.\frac{d}{dQ}\left\langle\frac{1}{r_{12}^3}-\frac{3z_{12}^2}{r_{12}^5}\right\rangle\right|_0 \approx 6.2 \text{ MHz/GPa}. \quad (5)$$

This compares favorably to the observed ~15 MHz/GPa shift. Based upon this estimate, the change in the unpaired spin density maybe inferred,

$$\left.\frac{d\kappa}{dP}\right|_0 = \frac{1}{\gamma B}\left.\frac{d\kappa}{dQ}\right|_0 \approx 0.0012 \text{ GPa}^{-1}, \quad (6)$$

which corresponds to an entirely reasonable ~0.1% GPa^{-1} change in the spin density. Given the approximations made in the derivation of the D parameter expression (3) and the pressure shift estimates (5) and (6), it is clear that while the semiclassical molecular orbital calculation performed here provides a clear physical interpretation of the observed pressure shift, it also has limitations. Future *ab initio* calculations are required to provide a more quantitatively accurate model of the pressure shift, including the spin density variation with pressure [46]. Further experimental observations of the spin density can be achieved via the pressure shifts of the NV^- hyperfine interactions with local ^{13}C nuclear spins, which directly depend on the spin density at the ^{13}C nuclei [39].

Analogous to previous estimates of the field and thermal sensitivities of the NV^- ODMR, the estimated ODMR pressure sensitivity of a single NV^- center at room temperature is [18]

$$\eta_{gs} = \frac{1}{2\pi\frac{dD(P)}{dP}K\sqrt{T_2^*}} \sim 0.6 \text{ MPa}/\sqrt{\text{Hz}}, \quad (7)$$

where K accounts for experimental factors such as collection efficiency. Note that the typical single center room temperature values $K \sim 0.02$ and $T_2^* \sim 1$ μs were used in the above estimate. Although the pressure shift of the optical ZPL is much larger than the ODMR, the large homogeneous broadening of the optical ZPL at room temperature and beyond [47] ensures that the ODMR sensitivity is significantly better than the optical sensitivity. However, in the low temperature limit ($T \lesssim 12$ K), where narrow optical lines (~140 MHz) of engineered NV^- centers can be obtained [48], an optical sensitivity of $\eta_{op} \approx 68$ Pa/$\sqrt{\text{Hz}}$ is achieved.

We now consider the performance of the current NV^- metrology applications under different conditions. The estimated pressure sensitivity of the NV^- ODMR implies that changes in pressure of ~1 MPa can be detected after one second of averaging time. As the majority of current proposals for NV^- magnetometry and electrometry are targeted at ambient conditions, where pressure fluctuations of the order of ~1 MPa are very unlikely to occur over time scales of a second, the pressure sensitivity of the NV^- ODMR will not influence the performance of these current proposals. Even up to pressures of ~50 GPa, which are relevant to studies of high-pressure superconductivity and magnetic phase transitions using DACs [22–28], the pressure fluctuations can be controlled to less than ~10 kPa on time scales of seconds (estimated based on resistance changes at the insulator-metal transition [49]). Hence, the observed hydrostatic pressure shift implies that the current proposals of NV^- magnetometry and electrometry will retain much of their sensitivity in the extremes of pressure.

Furthermore, the NV^- ODMR offers a more sensitive means to measure high pressures than existing techniques. As employed in this work, the current technique of choice utilizes the optical transitions of ruby and has a typical accuracy of ~10 MPa [43]. The NV^- center's pressure sensitivity, its possible inclusion with the sample in the DAC and its capability to switch to magnetometry or electrometry modes (assuming pressure fluctuations are controlled to < 1 MPa on the timescale of seconds) undoubtedly make the NV^- center the ideal probe for high-pressure phenomena. One possible design is depicted in Fig. 2(b), where a thin diamond chip containing an array or ensemble of NV^- centers is placed on top of a high-pressure superconductor sample inside the DAC. Employing existing techniques of wide field NV^- magnetometry [50], the NV^- array can be switched between pressure and stress [51] sensing and magnetometry, offering an unprecedented means to monitor the pressure and image the magnetic phenomena occurring at the surface of the high-pressure superconductor.

High-pressure experiments were supported by DOE-BES under Grant No. DE-FG02-02ER45955. CVD diamond preparation was supported by DOE-NNSA under Grant No. DE-FC52-08NA28554. This work was also supported by the Australian Research Council Discovery Project (No. DP120102232) and Centre of Excellence for Quantum Computation and Communication Technology (Project No. CE110001027). L. P. McGuinness acknowledges support from the Alexander von Humboldt Foundation.

*marcus.doherty@anu.edu.au

[1] J. Wrachtrup and F. Jelezko, J. Phys. Condens. Matter **18**, S807 (2006).
[2] P. C. Maurer *et al.*, Science **336**, 1283 (2012).

[3] A. Beveratos, R. Brouri, T. Gacoin, A. Villing, J.-P. Poizat, and P. Grangier, Phys. Rev. Lett. **89**, 187901 (2002).

[4] A. Alleaume, F. Treussart, G. Messin, Y. Dumeige, J.-F. Roch, A. Beveratos, R. Brouri-Tualle, J.-P. Poisat, and P. Grangier, New J. Phys. **6**, 92 (2004).

[5] J. M. Taylor, P. Cappellaro, L. Childress, L. Jiang, D. Budker, P. R. Hemmer, A. Yacoby, R. Walsworth, and M. D. Lukin, Nat. Phys. **4**, 810 (2008).

[6] G. Balasubramanian, I. Y. Chan, R. Kolesov, M. Al-Hmoud, J. Tisler, C. Shin, C. Kim, A. Wojcik, P. R. Hemmer, A. Krueger, T. Hanke, A. Leitenstorfer, R. Bratschitsch, F. Jelezko, and J. Wrachtrup, Nature (London) **455**, 648 (2008).

[7] J. R. Maze, P. L. Stanwix, J. S. Hodges, S. Hong, J. M. Taylor, P. Cappellaro, L. Jiang, M. V. Gurudev Dutt, E. Togan, A. S. Zibrov, A. Yacoby, R. L. Walsworth, and M. D. Lukin, Nature (London) **455**, 644 (2008).

[8] V. M. Acosta, E. Bauch, A. Jarmola, L. J. Zipp, M. P. Ledbetter, and D. Budker, Appl. Phys. Lett. **97**, 174104 (2010).

[9] F. Dolde, H. Fedder, M. W. Doherty, T. Nöbauer, F. Rempp, G. Balasubramanian, T. Wolf, F. Reinhard, L. C. L. Hollenberg, F. Jelezko, and J. Wrachtrup, Nat. Phys. **7**, 459 (2011).

[10] J. H. Cole and L. C. L. Hollenberg, Nanotechnology **20**, 495401 (2009).

[11] L. T. Hall, J. H. Cole, C. D. Hill, and L. C. L. Hollenberg, Phys. Rev. Lett. **103**, 220802 (2009).

[12] D. Maclaurin, M. W. Doherty, L. C. L. Hollenberg, and A. M. Martin, Phys. Rev. Lett. **108**, 240403 (2012).

[13] M. Ledbetter, K. Jensen, R. Fischer, A. Jarmola, and D. Budker, Phys. Rev. A **86**, 052116 (2012).

[14] A. Ajoy and P. Cappellaro, Phys. Rev. A **86**, 062104 (2012).

[15] M. W. Doherty, N. B. Manson, P. Delaney, F. Jelezko, and L. C. L. Hollenberg, Phys. Rep. **528**, 1 (2013).

[16] G. Balasubramanian *et al.*, Nat. Mater. **8**, 383 (2009).

[17] L. M. Pham, N. Bar-Gill, C. Belthangady, D. L. Sage, P. Cappellaro, M. D. Lukin, A. Yacoby, and R. L. Walsworth, Phys. Rev. B **86**, 045214 (2012).

[18] D. M. Toyli, D. J. Christle, A. Alkauskas, B. B. Buckley, C. G. Van de Walle, and D. D. Awschalom, Phys. Rev. X **2**, 031001 (2012).

[19] V. M. Acosta, E. Bauch, M. P. Ledbetter, A. Waxman, L.-S. Bouchard, and D. Budker, Phys. Rev. Lett. **104**, 070801 (2010).

[20] V. M. Acosta, A. Jarmola, L. J. Zipp, M. P. Ledbetter, E. Bauch, and D. Budker, Proc. SPIE Int. Soc. Opt. Eng. **7948**, 79480W (2011).

[21] X.-D. Chen, C.-H. Dong, F.-W. Sun, C.-L. Zou, J.-M. Cui, Z.-F. Han, and G.-C. Guo, Appl. Phys. Lett. **99**, 161903 (2011).

[22] V. V. Struzhkin, E. Gregoryanz, H. K. Mao, R. J. Hemley, and Y. A. Timofeev, in *High Pressure Phenomena*, edited by R. J. Hemley *et al.* (IOS Press/Societ Italiana di Fisica, Amsterdam, 2002).

[23] J.-F. Lin, V. V. Struzhkin, S. D. Jacobsen, M. Y. Hu, P. Chow, J. Kung, H. Liu, H.-K. Mao, and R. J. Hemley, Nature (London) **436**, 377 (2005).

[24] H. Takahashi, K. Igawa, K. Arii, Y. Kamihara, M. Hirano, and H. Hosono, Nature (London) **453**, 376 (2008).

[25] X. J. Chen, V. V. Struzhkin, Y. Yu, A. F. Goncharov, C.-T. Lin, H.-k. Mao, and R. J. Hemley, Nature (London) **466**, 950 (2010).

[26] L. Sun *et al.*, Nature (London) **483**, 67 (2012).

[27] I. A. Kornev, L. Bellaiche, P. Bouvier, P.-E. Janolin, B. Dkhil, and J. Kreisel, Phys. Rev. Lett. **95**, 166804 (2005).

[28] M. Ahart, H.-K. Mao, R. E. Cohen, R. J. Hemley, G. A. Samara, Y. Bing, Z.-G. Ye, and S. Kojima, J. Appl. Phys. **107**, 074110 (2010).

[29] X.-F. He, N. B. Manson, and P. T. H. Fisk, Phys. Rev. B **47**, 8816 (1993).

[30] S. Felton, A. M. Edmonds, M. E. Newton, P. M. Martineau, D. Fisher, D. J. Twitchen, and J. M. Baker, Phys. Rev. B **79**, 075203 (2009).

[31] J. A. Larsson and P. Delaney, Phys. Rev. B **77**, 165201 (2008).

[32] A. Gali, M. Fyta, and E. Kaxiras, Phys. Rev. B **77**, 155206 (2008).

[33] M. W. Doherty, N. B. Manson, P. Delaney, and L. C. L. Hollenberg, New J. Phys. **13**, 025019 (2011).

[34] J. R. Maze, A. Gali, E. Togan, Y. Chu, A. Trifonov, E. Kaxiras, and M. D. Lukin, New J. Phys. **13**, 025025 (2011).

[35] G. Davies and M. F. Hamer, Proc. R. Soc. A **348**, 285 (1976).

[36] L. J. Rogers, S. Armstrong, M. J. Sellars, and N. B. Manson, New J. Phys. **10**, 103024 (2008).

[37] V. M. Acosta, A. Jarmola, E. Bauch, and D. Budker, Phys. Rev. B **82**, 201202(R) (2010).

[38] N. B. Manson, L. Rogers, M. W. Doherty, and L. C. L. Hollenberg, arXiv:1011.2840v1.

[39] J. H. N. Loubser and J. A. van Wyk, Rep. Prog. Phys. **41**, 1201 (1978).

[40] N. B. Manson, J. P. Harrison, and M. J. Sellars, Phys. Rev. B **74**, 104303 (2006).

[41] See Supplemental Material at http://link.aps.org/supplemental/10.1103/PhysRevLett.112.047601 for experimental details and the semiclassical model of the ODMR pressure shift.

[42] H. K. Mao, J. Xu, and P. M. Bell, J. Geophys. Res. **91**, 4673 (1986).

[43] S. Klotz, J.-C. Chervin, P. Munsch, and G. Le Marchand, J. Phys. D **42**, 075413 (2009).

[44] M. Kobayashi and Y. Nisida, Jpn. J. Appl. Phys. **32**, 279 (1993).

[45] M. W. Doherty, F. Dolde, H. Fedder, F. Jelezko, J. Wrachtrup, N. B. Manson, and L. C. L. Hollenberg, Phys. Rev. B **85**, 205203 (2012).

[46] F. Neese and M. L. Munzarová, in *Historical Aspects of EPR Parameter Calculations*, edited by M. Kaupp, M. Bühl, and V. G. Malkin (Wiley-VCH, Weinheim, 2004).

[47] K.-M. C. Fu, C. Santori, P. E. Barclay, L. J. Rogers, N. B. Manson, and R. G. Beausoleil, Phys. Rev. Lett. **103**, 256404 (2009).

[48] A. Stacey, D. A. Simpson, T. J. Karle, B. C. Gibson, V. M. Acosta, Z. Huang, K. M. C. Fu, C. Santori, R. G. Beausoleil, L. P. McGuinness, K. Ganesan, S. Tomljenovic-Hanic, A. D. Greentree, and S. Prawer, Adv. Mater. **24**, 3333 (2012).

[49] A. G. Gavriliuk, V. V. Struzhkin, I. S. Lyubutin, S. G. Ovchinnikov, M. Y. Hu, and P. Chow, Phys. Rev. B **77**, 155112 (2008).

[50] S. Steinert, F. Dolde, P. Neumann, A. Aird, B. Naydenov, G. Balasubramanian, F. Jelezko, and J. Wrachtrup, Rev. Sci. Instrum. **81**, 043705 (2010).

[51] F. Grazioso, B. R. Patton, P. Delaney, M. L. Markham, D. J. Twitchen, and J. M. Smith, arXiv:1110.3658.